Fabrication by Electrodeposition: Building 3D Structures and Polymer Actuators

John D. Madden, Serge R. Lafontaine, and Ian W. Hunter

Department of Mechanical Engineering
Massachusetts Institute of Technology
77 Massachusetts Avenue, Cambridge MA 02139
USA

Abstract: Electrochemical deposition has traditionally been employed to grow metal coatings (plating) and to fill molds (electroforming). However, by localizing electric field or inducing local convection on a conducting substrate it is possible to write patterns without employing masks or molds. Here we present techniques capable of depositing high aspect ratio, truly 3D structures such as columns and helical springs.

Conducting polymers such as polyaniline, polyacetylene, and polypyrrole are routinely employed to fabricate batteries, capacitors, colour displays, and transistors. Here we demonstrate the electrodeposition of polypyrrole films to form bilayer actuators.

1. Introduction

Many materials can be electrodeposited, including pure metals, metal alloys [1], polymers and even some semiconductors [2]. Efforts to build and repair integrated circuits have led to methods of electrochemically depositing and etching micrometer and sub–micrometer wide lines of metals [3][4][5], polymers [6] and semiconductors [7]. High local deposition rates, up to 20μm/s, have been achieved with good deposit quality by increasing local mass transport using forced convection [8] or heat induced micro–stirring [5]. In this paper we will present two relatively new applications of electrochemical deposition, namely the fabrication of truly 3D microstructures [9] the growth of polymeric actuators [10][11][12].

2. Three Dimensional Local Electrodeposition

2.1 Concept

The concept of 3D local electrodeposition is outlined in Figure 1. Electric field and thus deposition are localized on a substrate by placing an electrode near the substrate surface. A potential applied between the substrate and the electrode through a plating solution generates the field and drives deposition. Movement of the electrode relative to the deposit allows three dimensional structures to be formed.

2.2 Implementation of Localized Electrodeposition

Figure 2 is a schematic diagram of the implementation. The electrode is an electrochemically etched tip coated with epoxy or glass. A sulfamate plating solution is used to deposit nickel. Details are given in reference [9]. Micro–stepping

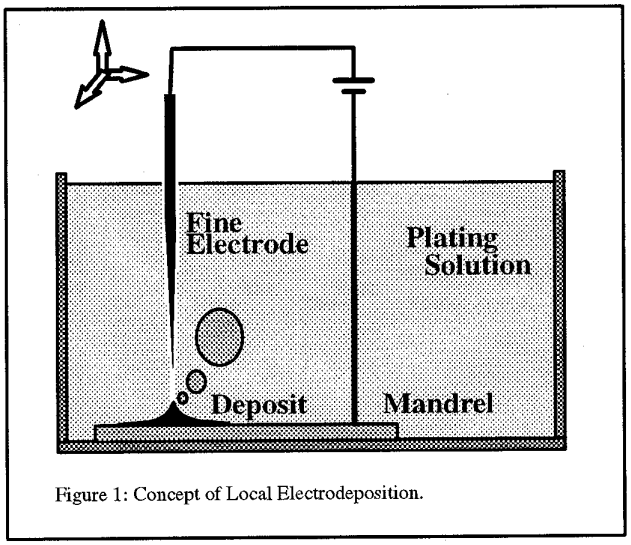

Figure 1: Concept of Local Electrodeposition.

motors (20 nm step size, Compumotor LN series) move the electrode in 3D. Current is read by a current amplifier (Keithley 428) and transmitted as a voltage to an A/D (HP E1413A). Step commands are sent to the microstepping drives via a digital I/O (C&H VXI441C), while potential is applied using a D/A (Tasco TVXI/DAC16) through a unity gain buffer. The apparatus is under software control on an IBM RS/6000 320.

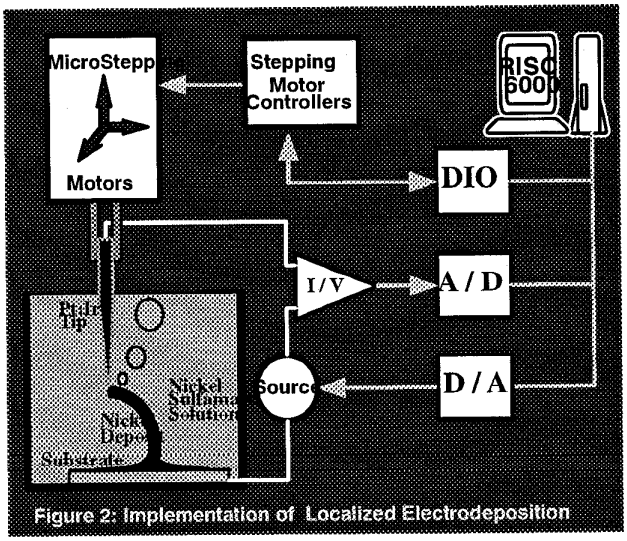

Figure 2: Implementation of Localized Electrodeposition

Sixth International Symposium on
Micro Machine and Human Science
0-7803-2676-8/95 $4.00 ©1995 IEEE.

Deposition is driven either in open loop, where the electrode is sent on a specified 3D trajectory at constant speed, or under current feedback control. In feedback mode, motion is signalled by a jump in current associated with contact between the growing deposit and the electrode. Figure 3 shows the measured step rise in current on contact.

2.3 Nickel Structures

Figure 4 shows a 1 mm diameter nickel spring grown in open loop mode at a rate of 6 μm/s. A similar spring has been shown to have spring constants of 1.3 kN/m and to be polycrystalline [9].

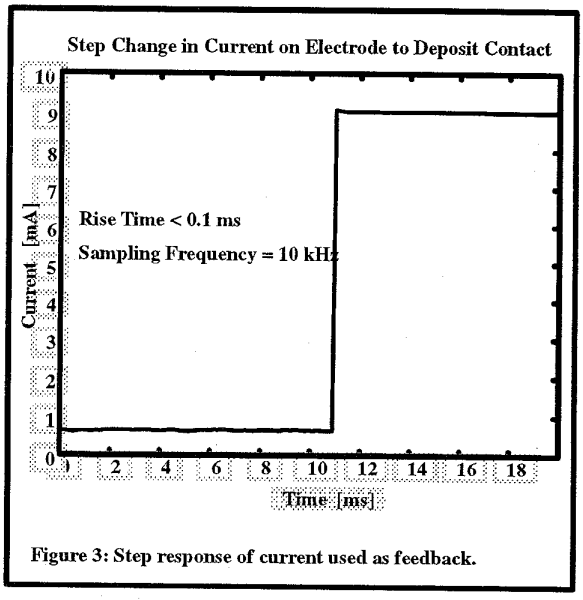

Figure 3: Step response of current used as feedback.

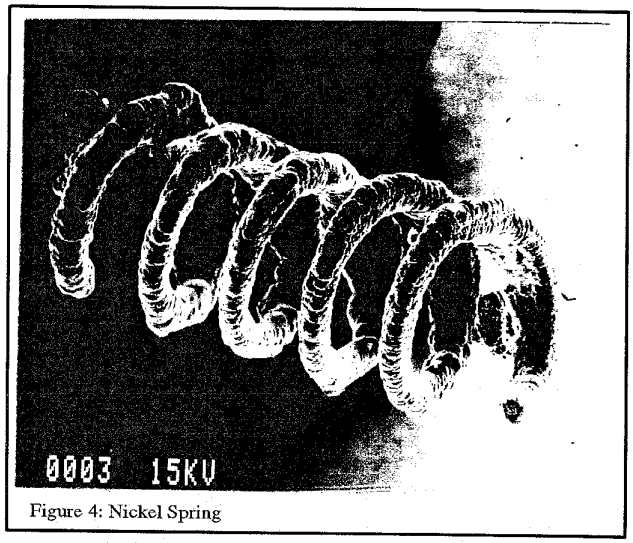

Figure 4: Nickel Spring

Figure 5 demonstrates the aspect ratio that can be achieved using this technique. The two columns shown are 45 μm in diameter. The left hand column is 1,600 μm tall, while the right hand column stands 7100 μm above the gold pads on which they are deposited. Growth rates varied between 1 and 1.5 μm/s. They were grown under feedback control, resulting in a much smoother surface finish than is achieved in open loop.

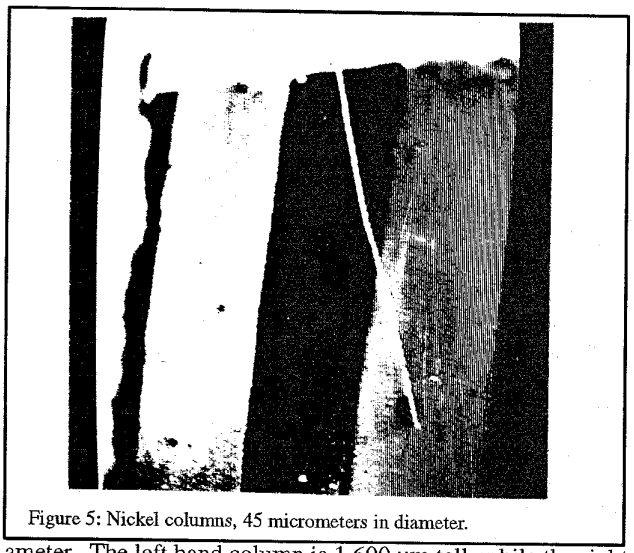

Figure 5: Nickel columns, 45 micrometers in diameter.

As with other truly 3D microfabrication methods, such as Micro–Stereo–Lithography [13] and Laser Chemical Vapour Deposition [14], localized electrodeposition promises to allow low cost, truly 3D microfabrication. The advantage of localized deposition is the wealth of materials available, including many metals, metal alloys, some polymers and semiconductors. Furthermore etching can be used allowing a combination of machining and etching. We expect to be able to reach sub–micrometer resolution with this technique given that this has been reached in 2D [3] [4].

3. Conducting Polymer Actuators

3.1 Concept

Conducting polymers, as their name implies, exhibit high electrical conductivity, which can even approach that of copper [12]. They also exhibit other properties valuable to the micro–system designer. By changing polymer oxidation state, conductivity can be switched by 11 orders of magnitude, an effect that has been employed to build kHz frequency transistors [15] and super–capacitors. Colour changes and light emission can also accompany oxidation and reduction, as can dimensional changes. High energy density batteries ($\approx$1 MJ/m^3) employ the high ion storage capability of the polymers. Common conducting polymers are polyaniline, polyphenylene, polythiopnene, polyacetylene and polypyrrole.

Volume changes associated with changes in oxidation states are taken advantage of to produce actuators. These volume changes are often related to the migration of ions in (and out) of the polymer doping (and undoping) [10] leading to ex-

pansions (and contractions) of the polymer. Calculations indicate that conducting polymers should be capable of producing stresses comparable to those generated by shape memory alloys, namely on the order of 180 MN/m^2, and strains of greater than 2% [16].

Much of the groundwork in fabricating and evaluating polymeric actuators has been performed at the Linköping Institute of Technology in Sweden by Drs. Smela, Inganäs, Pei and their co–workers [10][11][12]. In the following sections we demonstrate that electrochemically activated rates of contraction can be significantly enhanced by driving the potential higher and thus increasing reaction rate.

3.2 Implementation – Polymer Bilayer Actuator

In order to test the properties of conducting polymer actuators we chose to build a bilayer actuator. Polypyrrole was chosen for electrodeposition because it is relatively stable in air, and the reagents are not harmful and thus require few special precautions.

Mylar tape (CHR, New Haven CT) is employed as one half of the bilayer. A 50nm titanium adhesion layer followed by a 250 nm Pt film were electron–beam evaporated onto the tape. The strip of tape used was 3.3 mm wide by 75 mm long by 32 μm thick.

In the fabrication procedure, pyrrole is galvanostatically polymerized onto the Pt from a 0.1M pyrrole, 0.1M Na Dodecylbenzenesulfonate solution (DBS). The applied current was 150 nA, resulting in a potential across the cell of 0.83V. The counter electrodes used in these experiments are stainless steel, and are generally given surface areas > 20 times those of the working electrodes. 17 hours of deposition produced a black 61 μm thick film.

During deposition the large DBS anion is essentially locked into the depositing polymer structure, while the smaller sodium ion is free to move. In its oxidized state polypyrrole (PPy) is positively charged. The entrapped DBS serves to neutralize the film. When sufficiently negative potentials are applied between the Pt working electrode and the stainless steel counter electrode units of the polymer chain, designated P, are reduced:

$$P^+ + e^- \rightarrow P^o \qquad (1)$$

In order to maintain charge balance Na^+ ions enter the polymer. Note that if the DBS anions were of similar size to the sodium they would simply leave as the sodium was entering, producing no change in volume. By staying entangled in the polymer the DBS stays fixed and sodium ions dope the polymer, thereby increasing its volume. Contraction takes place when the polymer is oxidized and the sodium leaves the film:

$$P^o \rightarrow P^+ + e^- \qquad (2)$$

Typically a potential of –0.85V is employed to induce reduction and 0.3V for oxidation in a 0.1 M salt solution [11]. Contraction and expansion times for such applied potentials are about 60 s for a 5 mm displacement of a 30 micrometer thick PPy/200 nm Au/ 150 micrometer polyethylene trilayer, 50 mm long and 2mm wide.

We are able to achieve significantly faster response times by increasing the driving potential. Figure 6 shows the deflection of the multilayer from equilibrium position, Figure 6(a), to an intermediate position, Figure 6(b), and finally to a fully deflected state, Figure 6(c). Applying a potential of 2.5V, deflection from position (a) to (b) takes 20s, while further contraction of the polymer to state (c) takes another 52s. The current drawn ranged from 4.4mA at the beginning of the contraction to 3mA in the fully coiled state. The time to straighten is similar to the coiling time given the same average current. However a greater magnitude of potential is required (e.g. –3V to drive –2.5mA). The danger of increasing applied potentials is that the material may degrade more rapidly, in part due to dislodging of the bulky anions. This possibility has yet to be investigated.

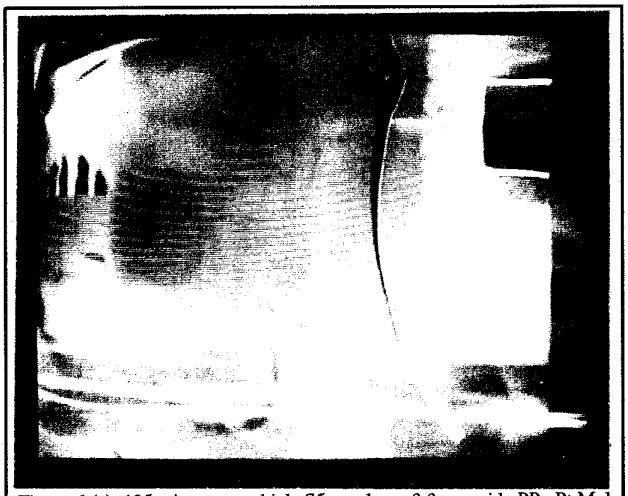

Figure 6 (a): 125 micrometer thick, 75 mm long, 3.3mm wide PPy:Pt:Mylar Laminate.

The coefficient of linear expansion, α, can be determined from the radius of curvature of the multilayer, 1/R, the layer thickness, h_1 (polypyrrole) and h_2 (mylar) and the Young's Moduli, E_1 (assume PPy similar to polyaniline, i.e. 5–9 GPa [17]) and E_2 (Mylar 3 GPa [18]) using the relation:

$$\frac{1}{R} - \frac{1}{R_o} = \frac{6\alpha}{\frac{(E_1h_1^2 - E_2h_2^2)^2}{E_1E_2h_1h_2(h_1+h_2)} + 4(h_1 + h_2)} . \qquad (3)$$

This yields a linear expansion coefficient, $\alpha = 0.017$, and a corresponding volume expansion of 0.052.

Raising the current to 7mA further increases deflection rate. With 8V applied between the multilayer and the counter electrode deflection between positions (a) and (b) occurs in <5s, with the tip velocity surpassing 7 mm/s.

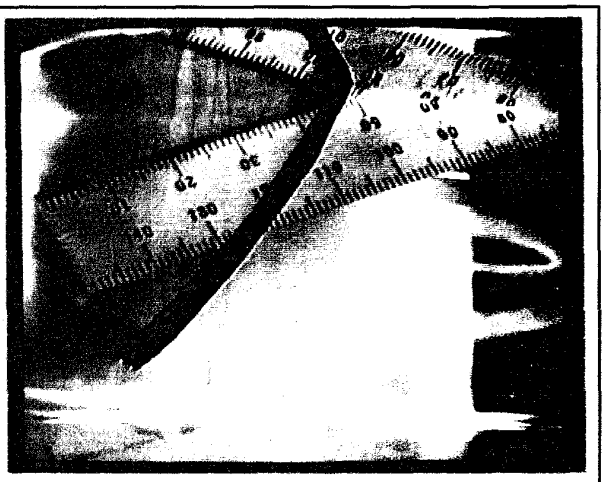

Figure 6 (b): Intermediate deflection of the bilayer.

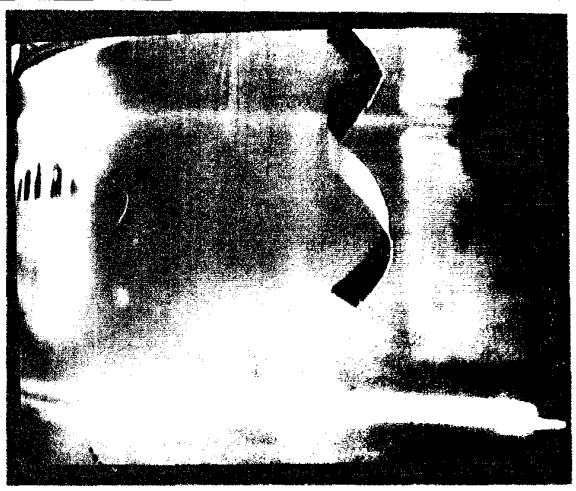

Figure 6 (c): Full contraction of the bilayer into a helix.

After several days of exposure to air the platinum film began delaminating from the mylar tape. A 0.75 mm wide by 7mm long by 32 μm thick strip was cut from the remaining polypyrrole/Pt bilayer and placed in 0.1M NaDBS solution, Figure 7.

Applying a 1Hz, 12V peak to peak square wave with a –2.5V DC offset induces a 2.5mA current and results in a 2 mm tip displacement, shown in Figure 7. At 14V p–p the amplitude increases to 2.4 mm. The amplitude is relatively constant below 1Hz, but decreases at higher frequencies. At 10 Hz the amplitude is about 1.2 mm, at 20 Hz, 0.6 mm and at 30 Hz roughly 0.05 mm. Note the bubbles visible in Figure 7. These are due to hydrolysis and possibly other reactions which become favourable at the elevated potentials employed. The bubbles emanate from the platinum side of the bilayer and the tip of the stainless steel tweezers used to anchor the actuator. Clearly high applied potential reduces efficiency as parasitic reactions

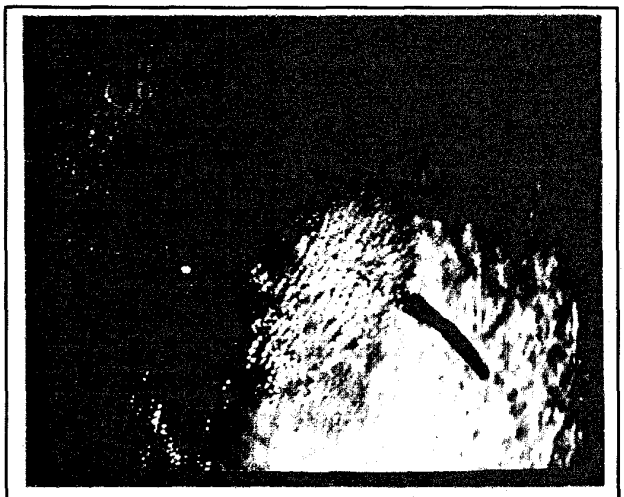

Figure 7: Deflection of PPy:Pt bilayer at 1 Hz.

are invoked. This effect could be drastically reduced by applying a thin insulating coating to the exposed platinum.

The bilayers can also be chemically activated. We have observed contraction and expansion by cycling between 0.1 M NaOH and 0.1 M HCl.

4. Acknowledgements

The authors wish to thank Peter Madden, Denzil Vaughan, Dr. Elizabeth Smela, and Colin Brenan for their valuable assistance and advice. The support of the U.S. Office of Naval Research and the Institute of Robotics and Intelligent Systems of Canada, one of the Canadian Networks of Centers of Excellence, is gratefully acknowledged.

5. References

[1] F.A. Lowenheim, *Electroplating*, New York: McGraw–Hill, 1978.

[2] Bard et.al., "High Resolution Deposition and Etching in Polymer Films", *U.S. Patent Number 4,968,390*, Nov. 6, 1990.

[3] J. Schneir et. al., "Creating and Observing Surface Features with a Scanning Tunneling Microscope", *SPIE* vol. 134, pp.1038–9, 1987.

[4] O.E.Husser, D.H.Craston and A.J.Bard, "Scanning Electrochemical Microscopy: High–Resolution Deposition and Etching of Metals", *Journal of the Electrochemical Society*, vol.136, pp.3222–9, 1989.

[5] J.C.Puippe, R.E.Acosta and R.J.von Gutfeld, "Investigation of Laser–Enhanced Electroplating Mechanisms", *Journal of the Electrochemical Society: Electrochemical Science and Technology*, vol. 128, pp.2539–2545, 1981.

[6] Y.–M. Wuu, F.–R.F. Fan and A.J. Bard, "High Resolution Deposition of Polyaniline on Pt with the Scanning Electrochemical Microscope", *Journal of the Electrochemical Society*, vol. 136, pp. 885–6 1989.

[7] C.W.Lin, F.–R.F.Fan and A.J.Bard, "High Resolution Photoelectrochemical Etching of n–GaAs with the Scanning Electrochemical and Tunneling Microscope", *Journal of the Elec-*

trochemical Society, vol.134, pp.1038–9, 1987.
[8] Gelchinski et.al., "Laser–enhanced Jet–Plating and Jet–Etching: High–Speed Maskless Patterning Method", *U.S. Patent Number 4,497,692*, Feb. 5, 1985.
[9] J.D.Madden and I.W.Hunter, "3D Micro–Fabrication by Localized Electrochemical Deposition", *Journal of Microelectromechanical Systems*, submitted 1995.
[10] E. Smela, O. Inganäs and I. Lundström, "Silicon Microfabrication + Conducting Polymers = New Devices", Proceedings of the ELBA Forum, Plenum Press, March 10–12, 1994.
[11] Q.Pei and O. Inganäs, "Conjugated Polymers and the Bending Cantilever Method: Electrical Muscles and Smart Devices", *Advanced Materials*, vol.4, pp.277–8, 1992.
[12] E.Smela, O. Inganäs and Q.Pei, "Electrochemical Muscles: Micromachining Fingers and Corkscrews", *Advanced Materials*, vol. 5, pp.630–632,
[13] K. Ikuta, K. HIrowatari, and T. Ogata, "Three Dimensional Micro Integrated Fluid Systems (MIFS) Fabricated by Stereo Lithography", *IEEE MEMS Conference*, pp. 1–6, 1994.
[16] I.W.Hunter and S.R.Lanfontaine, "A Comparison of Muscle with Artificial Actuators", *IEEE Sensors and Actuators*, pp.178–185, 1992.
[18] *Goodfellow Catalogue*, Goodfellow Corporation, Berwyn PA, p.425, 1994.